Supporting Information

Integrating metal framework with Co-confined carbon nanotubes as trifunctional electrocatalysts to boost electron and mass transfer approaching practical applications

Xiao Zhou,[ab,†] Xinyan Leng,[a,†] Cong Ling,[b] Hanbao Chong,[b] An-Wu Xu[b,*] and Zhengkun Yang[a,*]

[a]Institutes of Physical Science and Information Technology, Anhui Graphene Engineering Laboratory, Key Laboratory of Structure and Functional Regulation of Hybrid Materials (Anhui University), Ministry of Education, Hefei, 230601, China

[b]Hefei National Laboratory for Physical Sciences at the Microscale, University of Science and Technology of China, Hefei, 230026, China

Experimental Methods

***Material*:** Melamine, Cobalt (Co) foam (thickness: 0.2 mm) were purchased from Sinopharm Chemical Reagents, China. All of the chemicals used in this experiment were analytical grade and used without further purification.

***Synthesis of Co/N-CNTs catalysts*:** The Co/N-CNTs samples were prepared by direct pyrolysis of the melamine powder covered Co foam. In a typical procedure, the melamine (0.2, 0.3 and 0.5 g cm^{-2}) was sprayed on two surfaces of Co foam, and placed in a porcelain boat and annealed in N_2 flow at 1000 °C for 1 h with a ramping rate of 10 °C min^{-1}. The resultant Co/N-CNTs materials with different melamine loadings were defined as the Co/N-CNTs-1, Co/N-CNTs-2 and Co/N-CNTs-3 catalysts.

***Catalyst characterization*:** Powder X-ray diffraction patterns of samples were recorded on a Rigaku Miniflex-600 operating at 40 kV voltage and 15 mA current with Cu Kα radiation (λ=0.15406nm). The scanning electron microscope (SEM) was performed on JSM-6700F SEM. Transmission electron microscopy (TEM) images and the EDS mapping were obtained with a JEOL-2010 microscope at an accelerating voltage of 200 kV. Thermal gravimetric (TG) measurements were carried out on a ShimadzuTGA-50 analyzer at a heating rate of 10 ℃/min in the air. X-ray photoelectron spectroscopy (XPS) was collected on scanning X-ray microprobe (PHI 5000 Verasa, ULAC-PHI, Inc.) using Al Ka radiation and the C1s peak at 284.8 eV as an internal standard. Fourier Transform infrared (FTIR) spectra of the sample were performed using a Nicolet Nexus spectrometer. XAFS spectra at the Co K-edge were recorded at the 1W1B station of the Beijing Synchrotron Radiation Facility (BSRF), China. The Co-edge XANES data were recorded in a fluorescence mode. Co foil and CoO, Co_3O_4 were used as references. The storage

ring was working at the energy of 2.5 GeV. The hard X-ray was monochromatized with Si(111) double-crystals. The acquired EXAFS data were extracted and processed according to the standard procedures using the ATHENA module implemented in the IFEFFIT software packages. The k^3-weighted EXAFS spectra were obtained by subtracting the post-edge background from the overall absorption and then normalizing with respect to the edge-jump step. Near Edge X-ray Absorption Fine Structure (NEXAFS) were carried out at the Catalysis and Surface Science Endstation at the BL11U beamline and Photoemission endstation at the BL10B beamline in the National Synchrotron Radiation Laboratory (NSRL) in Hefei, China.

Electrochemical measurements: All electrochemical measurements were conducted on an electrochemical workstation (CHI 760E) with a conventional three-electrode configuration at room temperature. The Co/N-CNTs samples directly served as the working electrode, while the graphite rod and Ag/AgCl (saturated KCl) were used as the counter and reference electrodes, respectively. ORR tests were conducted in O_2-satuated 0.1 M KOH solution, while OER and HER tests were conducted in 1 M KOH electrolyte. The linear sweep voltammetry curves were recorded at a scan rate of 10 mV s^{-1}. The long-term stability test was performed using amperometric i-t curve method at a constant current density. Electrochemical impedance spectroscopy (EIS) measurements were carried out from 0.01 to 10^5 Hz to evaluate the charge-transfer ability of the catalysts. Electrochemical active surface area (ECSA) of catalysts was obtained from double-layer capacitance (C_{dl}) value, which was assessed by cyclic voltammetry (CV) recorded at different scan rates ranging from 2 mV s^{-1} to 10 mV $s^{-1}$with an interval point of 2 mV s^{-1}.

Rechargeable Zn-air battery measurements: The Zn-air batteries were performed in a home-built electrochemical cell. A polished Zn foil (thickness of 0.2 mm) was employed as the anode and the Co/N-CNTs as air cathode. And 6 M KOH containing 0.2 M $ZnCl_2$ was used as electrolyte. For comparion, Ccarbon paper-supported Pt/C+RuO_2 electrode was also prepared. Electrochemical reactors with total volume of 5 mL were constructed to test the Zn-air batteries. All the measurements were conducted on the as-constructed cell at room temperature with CHI 760E electrochemical workstation (Shanghai Chenhua, China). The charge-discharge cycle stability for Zn-air battery tested using a Land-CT2001A testing system.

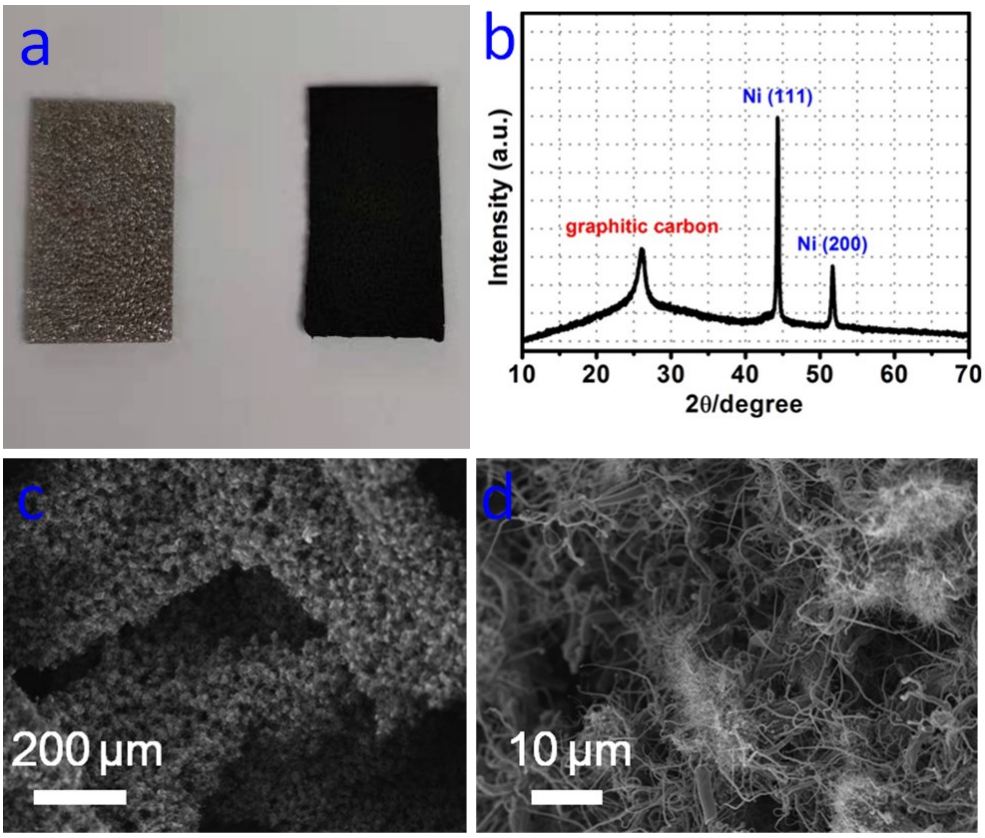

Figure S1 (a) Photos of the prepared Ni/N-CNTs. (b) XRD pattern of Ni/N-CNTs and (c, d) SEM images of the Ni/N-CNTs.

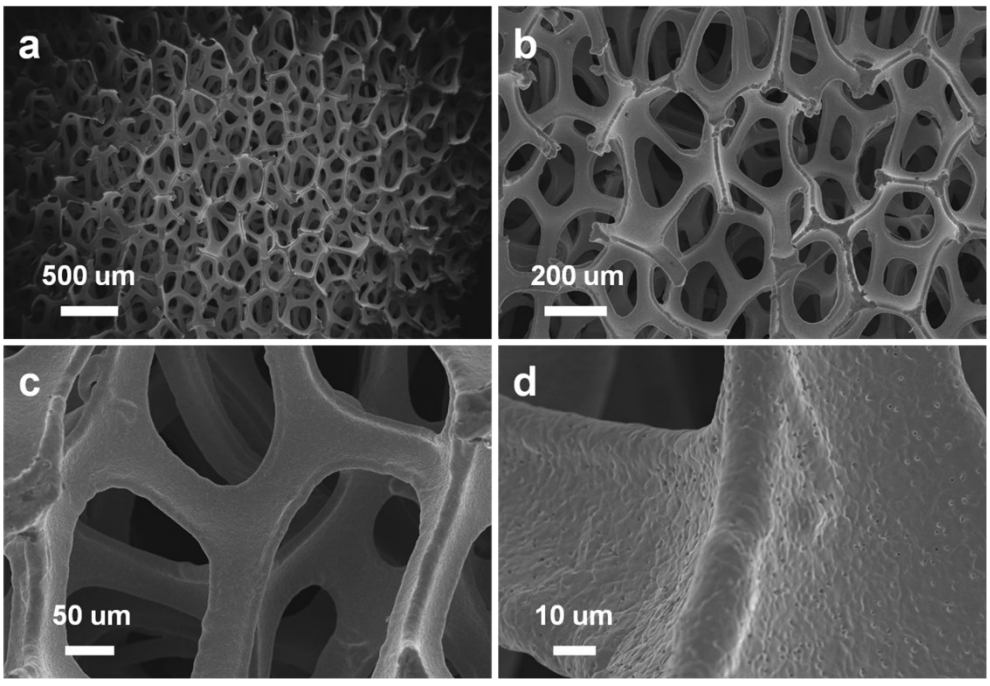

Figure S2. SEM images of pristine Co foam with different magnification.

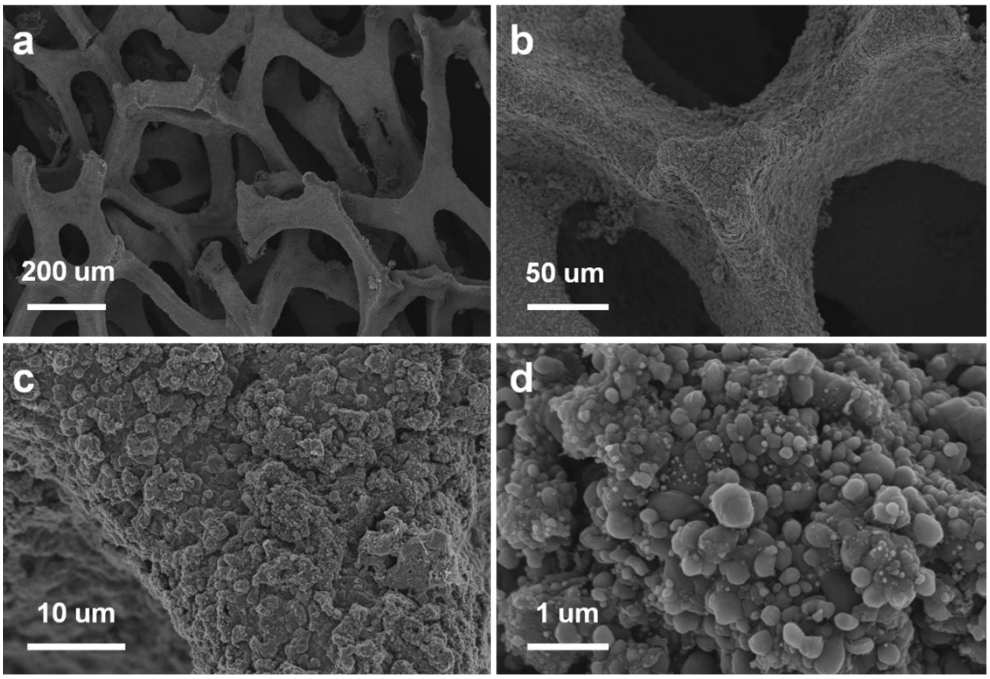

Figure S3. SEM images of as-prepared Co/N-CNTs-1 with different magnification.

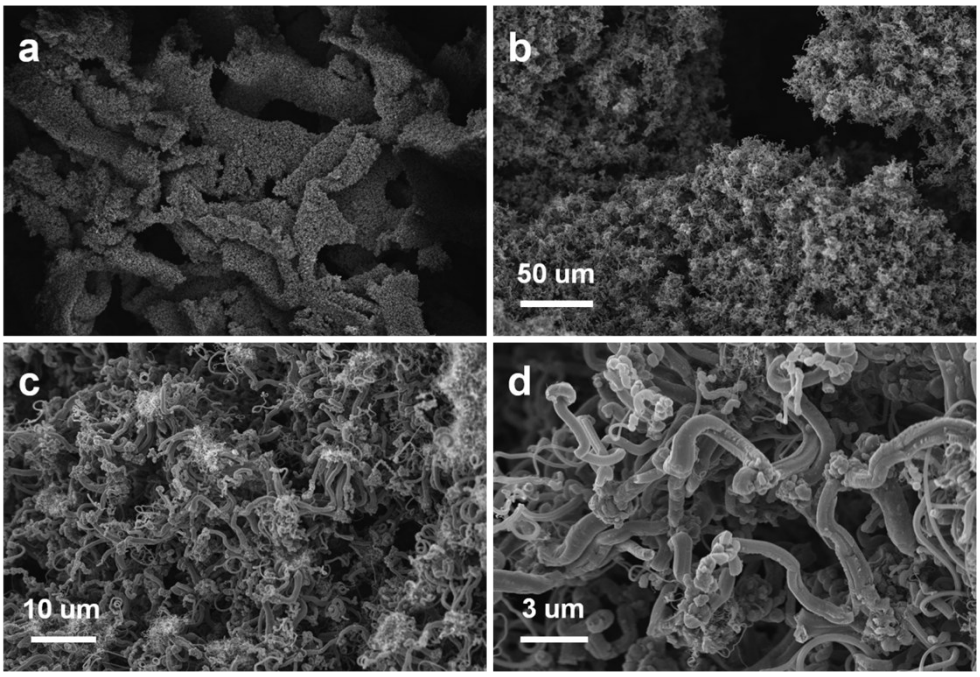

Figure S4. SEM images of as-prepared Co/N-CNTs-3 with different magnification.

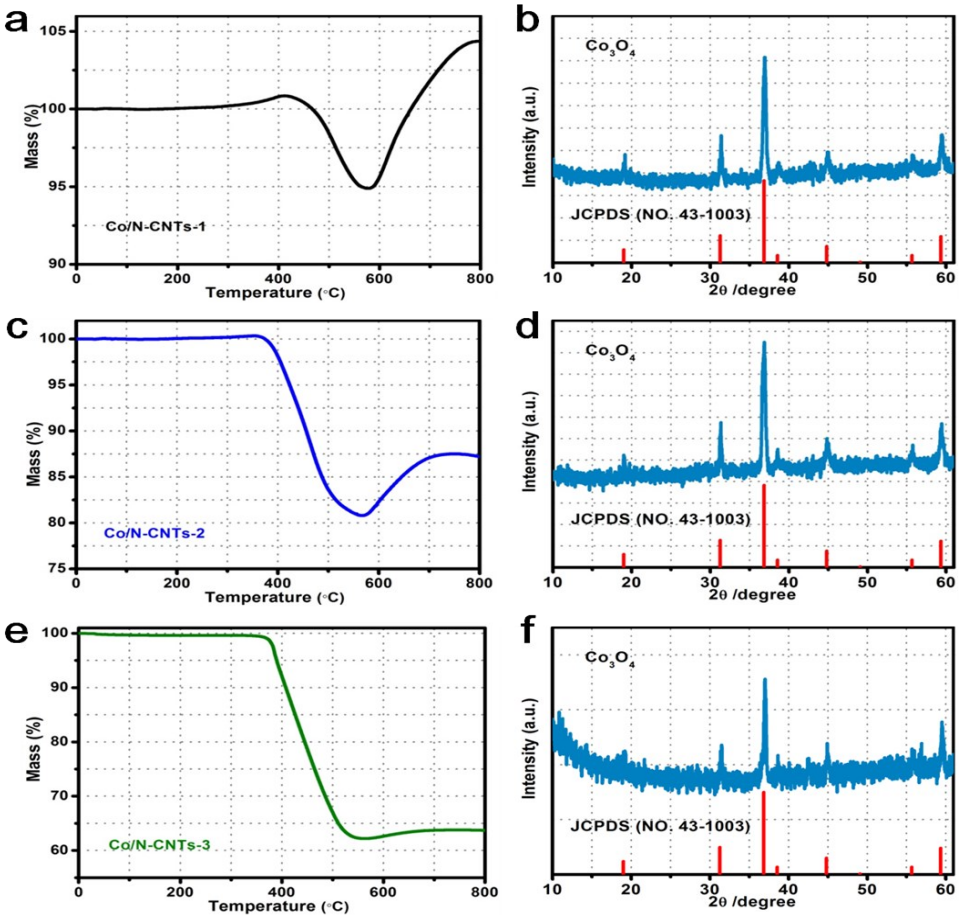

Figure S5. TGA analyses of the Co/N-CNTs catalysts and XRD patterns of the resulted powders from the Co/N-CNTs samples after combustion in air: (a, b) Co/N-CNTs-1, (c, d) Co/N-CNTs-2 and (e, f) Co/N-CNTs-3.

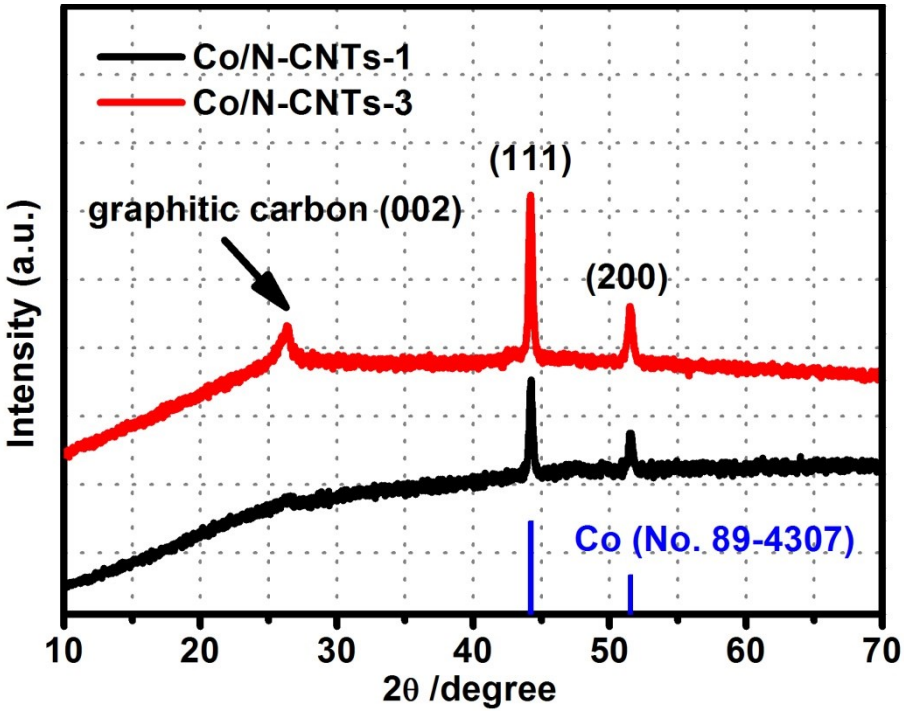

Figure S6. The XRD patterns of Co/N-CNTs-1 and Co/N-CNTs-3 sample.

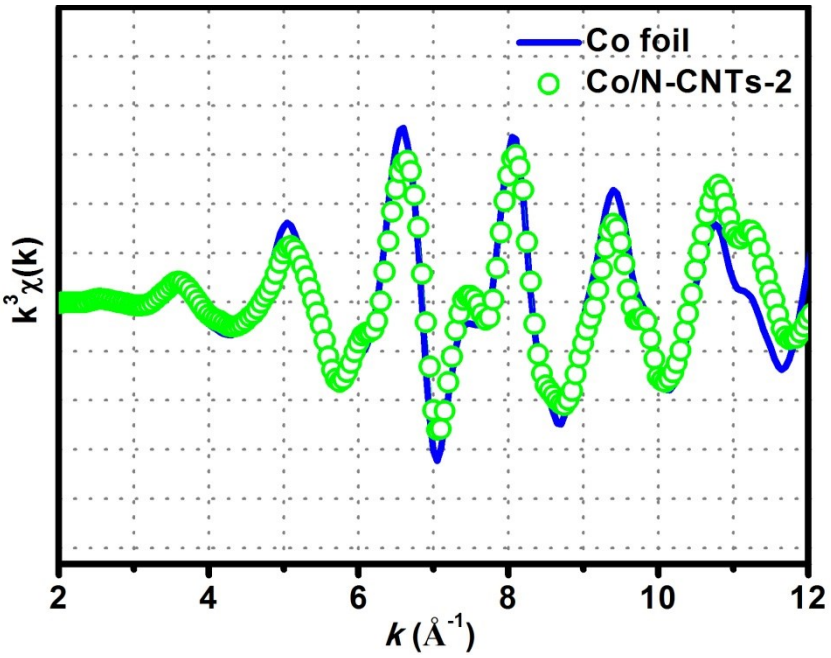

Figure S7. Co K-edge EXAFS spectra in *k*-space for the Co/N-CNTs-2 and Co foil samples.

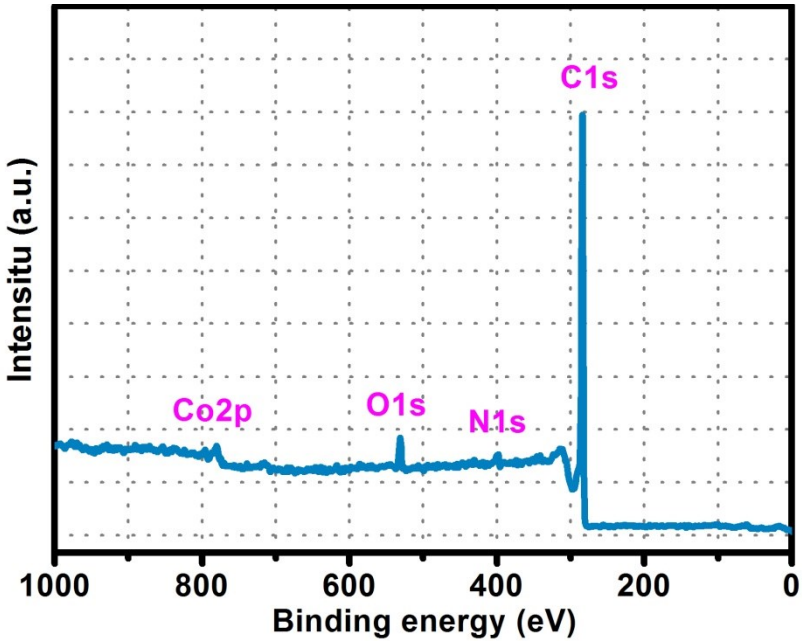

Figure S8. XPS survey scan of Co/N-CNTs-2 catalyst.

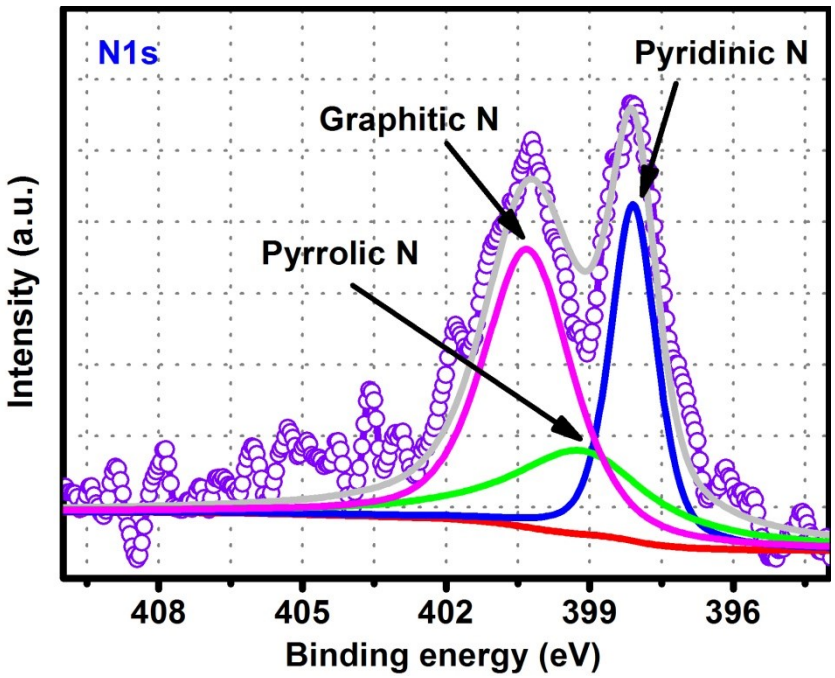

Figure S9. XPS spectrum for the N1s of the Co/N-CNTs-2 catalyst.

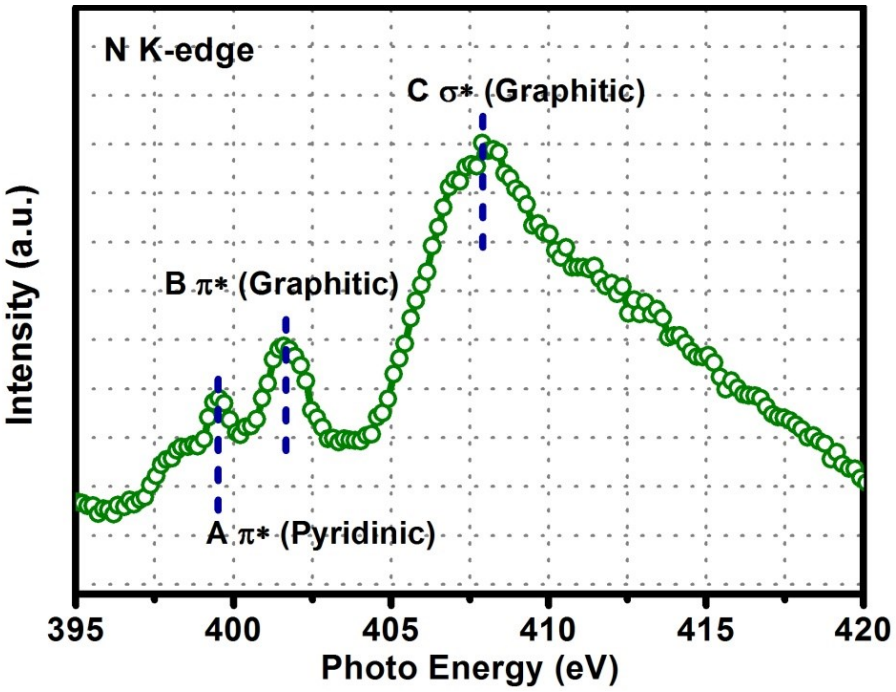

Figure S10. N K-edge NEXAFS spectrum of the Co/N-CNTs-2 catalyst.

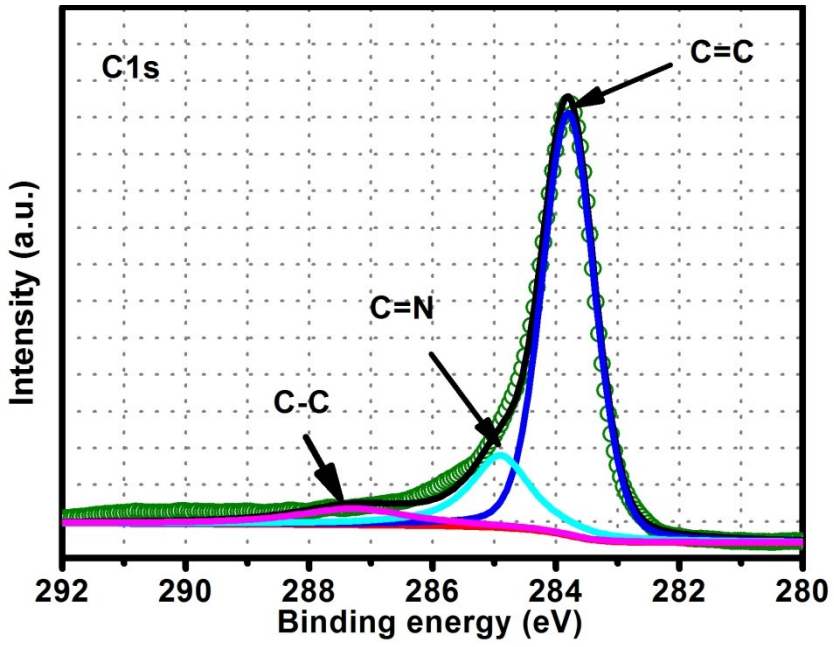

Figure S11. XPS spectrum for C1s of the Co/N-CNTs-2 catalyst.

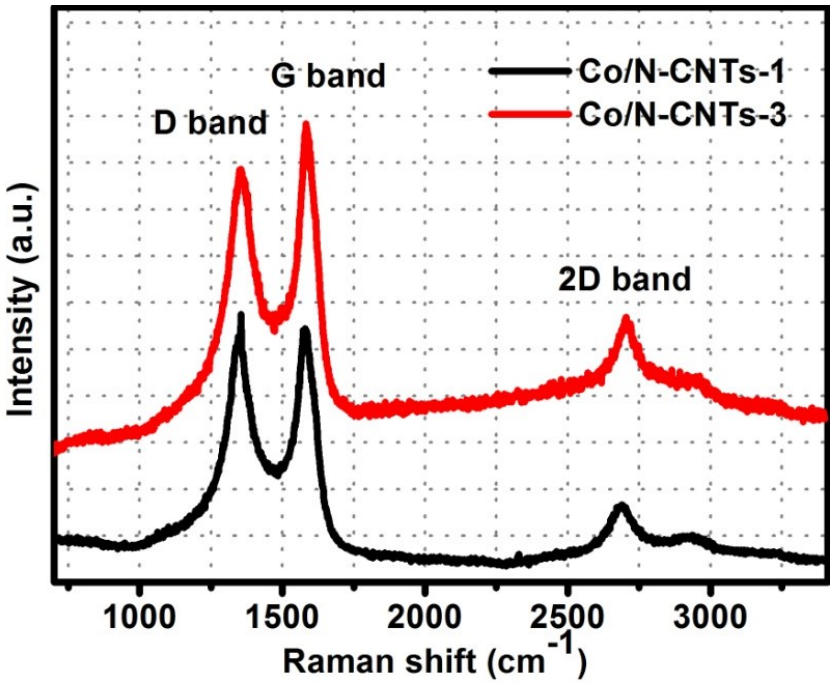

Figure S12. Raman spectra of Co/N-CNTs-1 and Co/N-CNTs-3 catalyst.

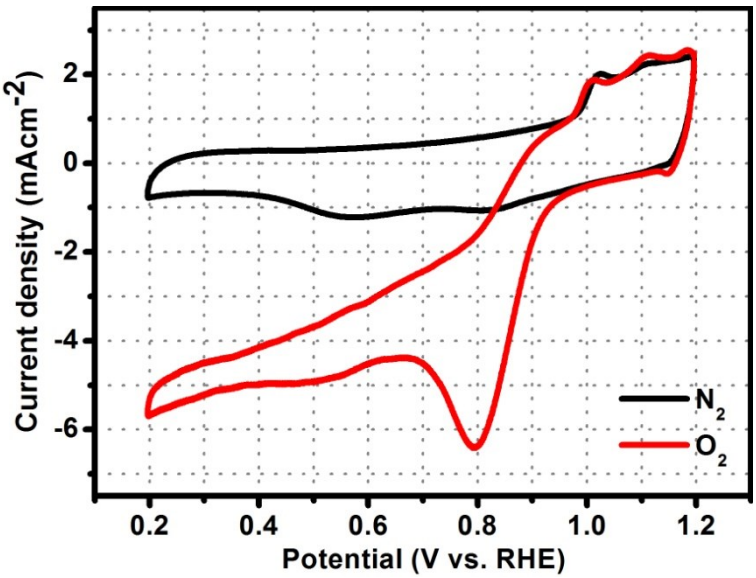

Figure S13. CV curves of the Co/N-CNTs-2 tested in both N_2-saturated and O_2-saturated 0.1 M KOH at 10 mV s^{-1}.

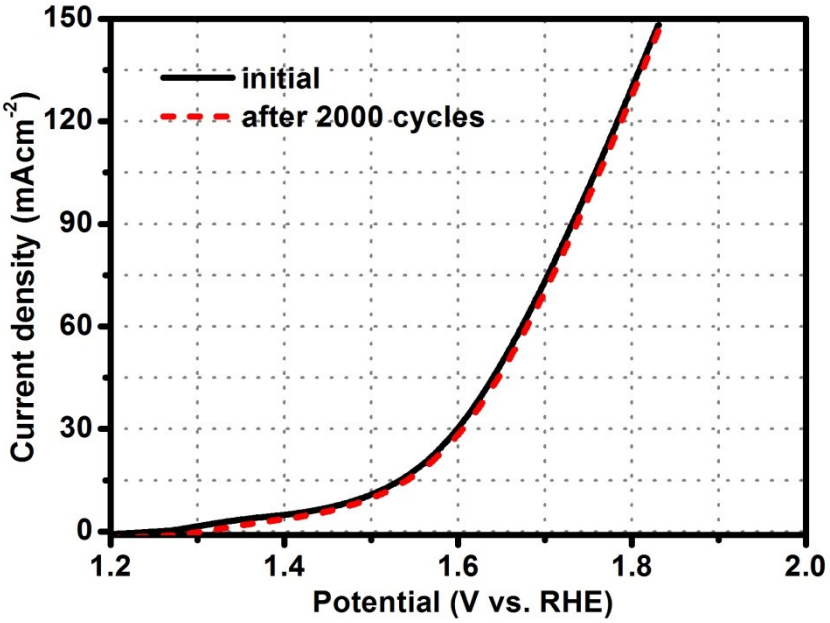

Figure S14. OER LSV curves recorded for Co/N-CNTs-2 before and after 2000 cycles.

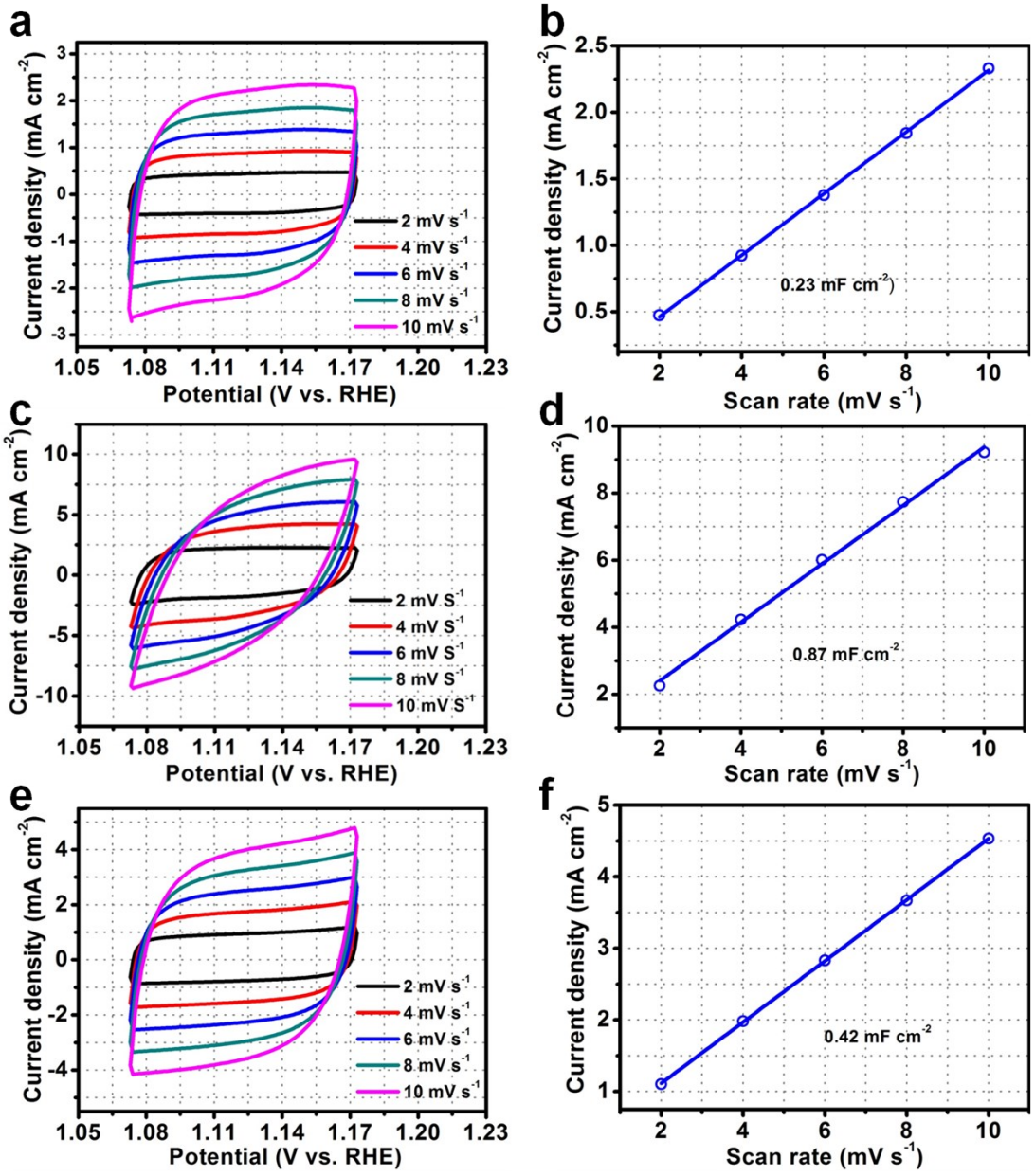

Figure S15. Cyclic voltammograms (CV) curves for (a) Co/N-CNTs-1, (c) Co/N-CNTs-2, (e) Co/N-CNTs-3 at various scan rates. The differences in current density variation ($\Delta j = ja - jc$) at the potential of 1.16 V vs.RHE plotted against scan rate of (b) Co/N-CNTs-1, (d) Co/N-CNTs-2, (f) Co/N-CNTs-3. The plot slope of current density against scan rate has a linear relationship was the double layer capacitance, which can be used to calculate the electrochemical surface area (ESCA) of (b) Co/N-CNTs-1, Co/N-CNTs-2 and Co/N-CNTs-3. The Co/N-CNTs-2 electrode has the larger active surface area and thus possesses more active sites and exposed edges for electrocatalysis.

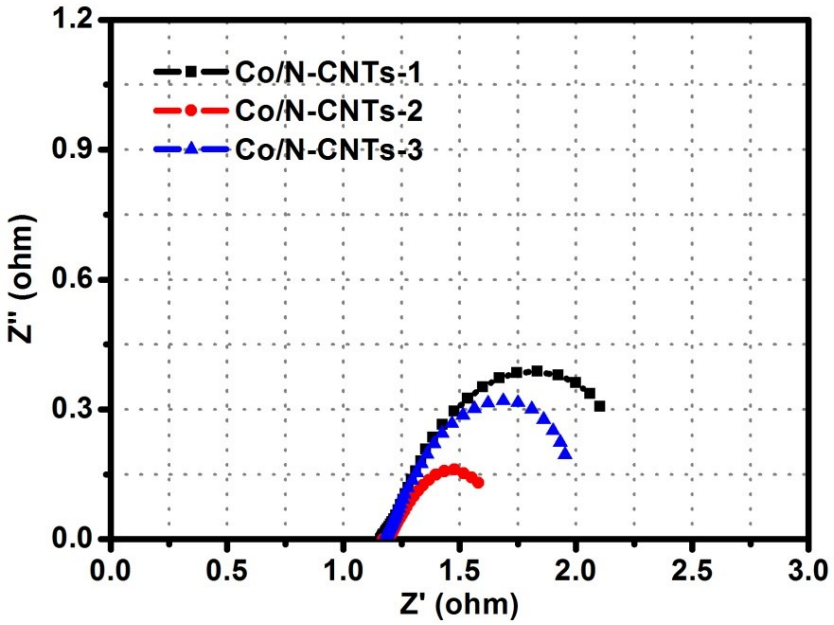

Figure S16. Electrochemical impedance spectroscopy (EIS) Nyquist plots for the Co/N-CNTs-1, Co/N-CNTs-2 and Co/N-CNTs-3 recorded at 1.55 V vs. RHE in OER.

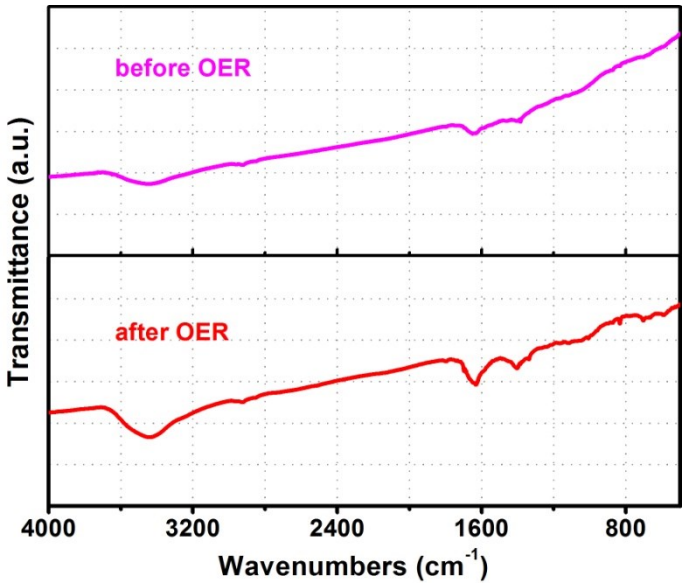

Figure S17. FTIR analysis of the Co/N-CNTs-2 sample before and after OER.

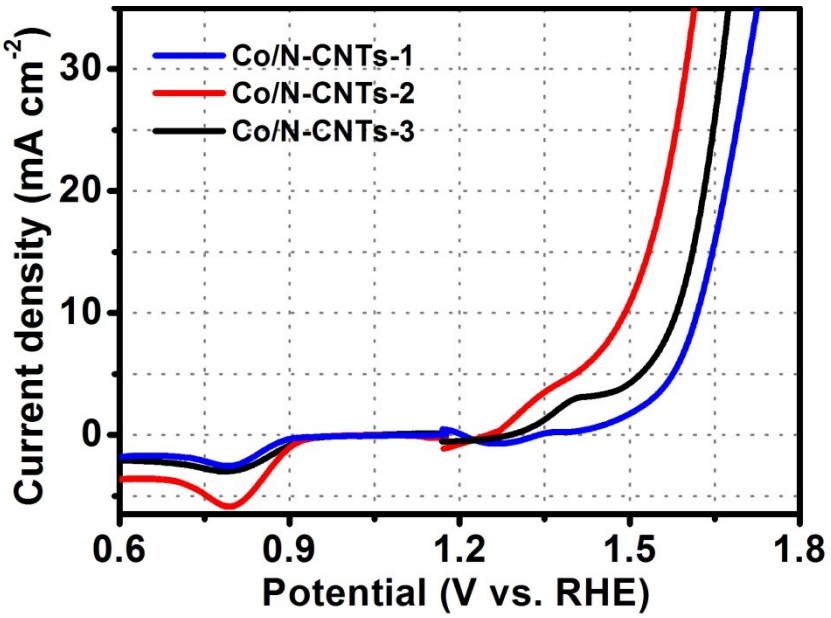

Figure S18. ORR and OER polarization curves of different catalyst electrodes.

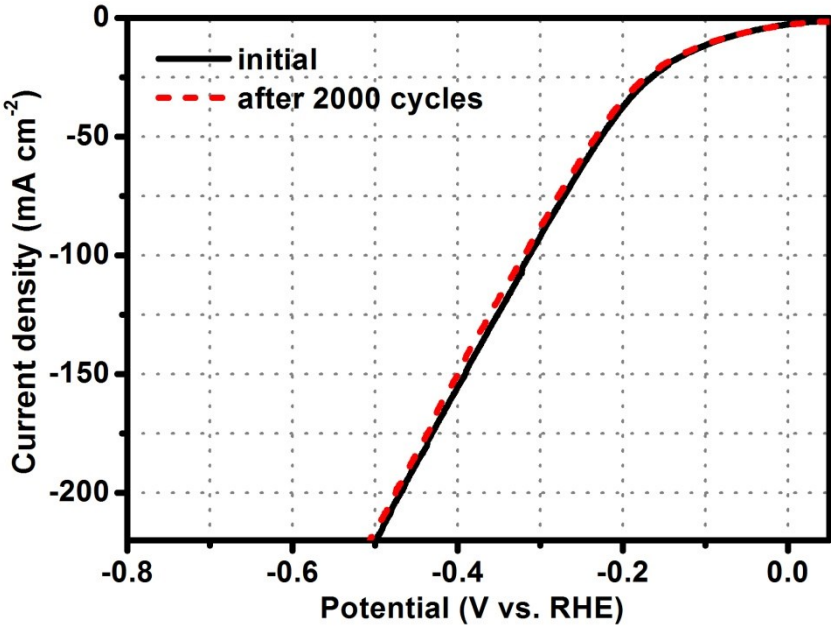

Figure S19. HER LSV curves recorded for Co/N-CNTs-2 before and after 2000 cycles.

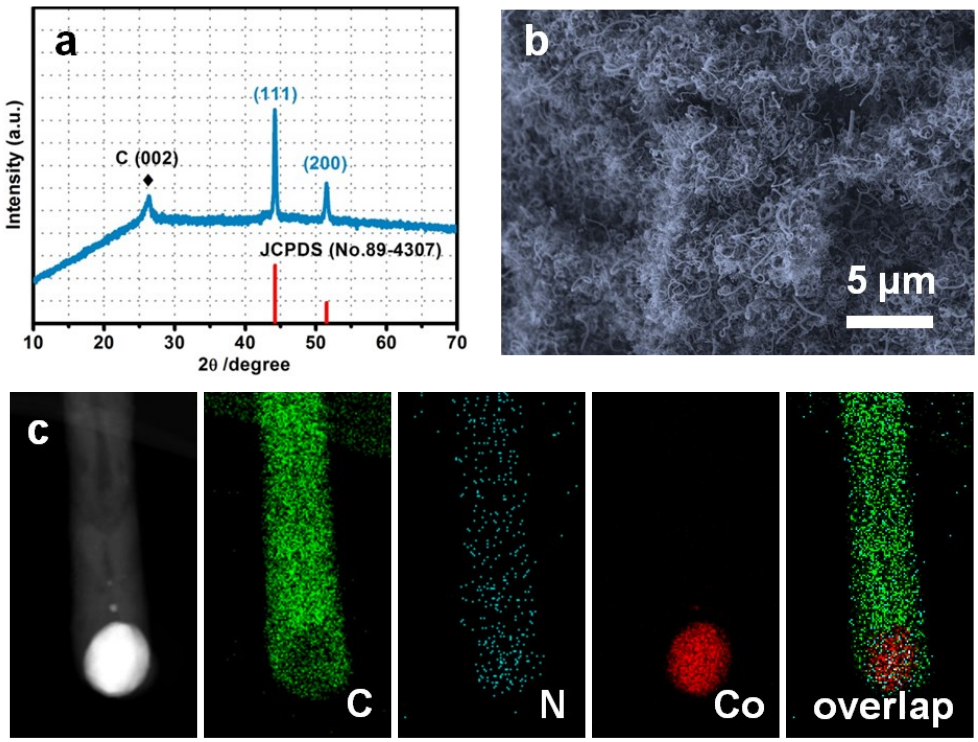

Figure S20. (a) XRD, (b) SEM, (c) Magnified HAADF STEM image and elemental mappings of Co/N-CNTs-2 catalyst after durability test.

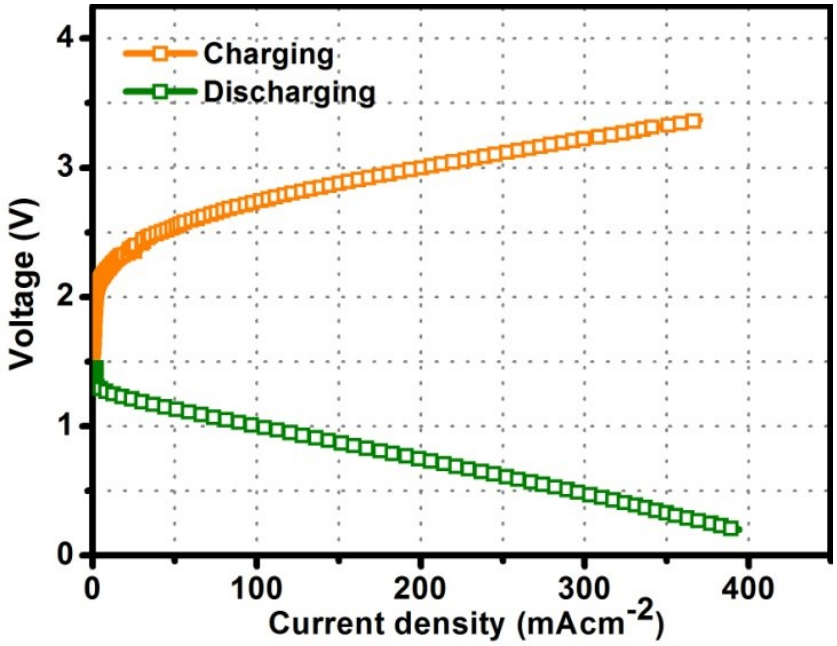

Figure S21. Discharging and charging profile of liquid Zn-air battery assembled from Co/N-CNTs-2 air-electrode.

Table S1. The Comparison of ORR performance of the Co-based material catalysts from the recent literature and this work (0.1 M KOH medium).

Catalysts	Haf-wave potential	Onset potential (V vs RHE)	Reference
Co/N-CNTs-2	0.863	0.98	This work
Co_2P/CoNPC	0.843	0.963	Adv. Mater. 2020, 2003649
CoP-CMP800	0.81	0.85	Adv. Mater., 2014, 26, 1450.
Co/N-carbon fibres	NA	0.95	Chem. Eur. J. 2015, 21, 2165.
CoP nanocrystals	0.8	0.67	Nano Lett. 2015, 15, 7616.
CoP nanoparticle	0.87	0.81	Adv. Energy Mater. 2018, 8, 1703623.
CoII-A-rG-O	0.81	0.88	Angew. Chem. Int. Ed., 2015, 54, 12622.
N/Co-doped PCP//NRGO	0.86	0.97	Adv. Funct. Mater. 2015, 25, 872.
rGO/($Co2^{+}$–THPP)$_7$	/	0.86	Angew. Chem. Int. Ed., 2013, 52, 5585.
Co–N–C–NS	0.84	0.93	Nanoscale, 2015, 7, 10334
CoMnP4 nanoparticles	0.89	0.78	J. Mater. Chem. A. 2018, 6, 11281.
Graphene/Co_3O_4	NA	0.95	Angew. Chem. Int. Ed. 2013, 52, 12105.
Co_3O_4/N-rmGO	0.83	0.88	Nat. Mater. 2011, 10, 780
Co-SAs@NC	0.96	0.82	Angew. Chem. Int. Ed., 2019, 131, 5413.
Co-N-C	0.871	0.98	ACS Catal.2015, 5, 7068.
Co@Co_3O_4/NC	0.8	NA	Angew. Chem. Int. Ed. 2016, 55, 1.

LDH@ZIF-67-800	0.83	0.94	Adv. Mater. 2016, 28, 2337.
Co@Co3O4@C-CM	0.83	0.91	Energy Environ. Sci. 2015, 8, 568.
P-CNCo-20	0.85	0.93	Adv. Mater. 2015, 27, 5010.
ZIF-67-900	0.85	0.91	J. Mater. Chem. A 2014, 2, 14064.
Co/N/rGO(NH_3)	0.81	0.85	J. Power Sources, 2013, 243, 65
CoO/NCNT	0.83	0.93	J. Am. Chem. Soc. 2012, 134, 15849.
GNPCSs-800	NA	0.957	Angew. Chem. Int. Ed. 2014, 53, 14235
Co−N/CNFs	0.82	0.92	ACS Catal. 2017, 7, 6864.
Co SAS/N-C(900)	0.881	0.98	Angew. Chem. Int. Ed. 2016, 55, 10800.
CoO/C	0.77	0.85	ACS Catal. 2014, 4, 2998
Co-ISAS/p-CN	0.97	0.838	Adv. Mater. 2018, 30, 1706508.
SC CoO	0.96	0.85	Nat. Commun. 2016, 7, 12876.

Table S2. The Comparison of OER performance of the Co-based material catalysts from the recent literature and this work (1 M KOH medium).

Catalysts	**η@10 mA/cm^2 (mV)**	**Tafel slop (mV/ dec)**	**Reference**
Co/N-CNTs-2	265	45	**This work**
Co_3O_4/$NiCo_2O_4$/GC	340	88	J. Am. Chem. Soc. 2015, 137, 5590.
Co/CNFs(1000)	320	79	Adv. Mater. 2019, 1808043

CoMnP nanoparticles	330	61	J. Am. Chem. Soc. 2016, 138, 4006.
NiCoP/C nanobox	330	96	Angew. Chem. Int. Ed. 2017, 56, 3955.
A-CoS4.6O0.6 PNCs	290	67	Angew. Chem. Int. Ed. 2017, 56, 4858.
CoP/rGO-400	340	66	Chem. Sci. 2016, 7, 1690.
CeO_2/$CoSe_2$	310	44	Small 2015, 11, 182.
Co_3O_4/SWNT	580	104	Nano Res. 2012, 5, 521.
Co@N-C	420	108	J. Mater. Chem. A 2014, 2, 20067.
Co-P	345	47	Angew. Chem. Int. Ed. 2015,54,6251.
Ni-Co phosphide	360	82	J. Mater. Chem. A 2016, 4, 7549.
Co-N,B-CSs	430	NA	ACS Nano 2018, 12, 1894.
Co_3O_4 NCs	320	116	Chem. Commun. 2015, 51, 8066.
CoP NR	490	84	ACS Catal. 2015, 5, 6874.
$NiCo_2O_4$ NNs	565	292	J. Phys. Chem. C 2014, 118, 25939.
Co_3O_4@N-rmGO	310	67	Nat. Mater. 2011, 10, 780.
$NiCo_2O_4$@MnO_2-CNTs	400	92	Nanoscale, 2018, 10, 13626.
Co_4N/CNW/CC	310	81	J. Am. Chem. Soc. 2016, 138, 10226.
Co_3O_4/Co_2MnO_4 nanocomposite	540	NA	Nanoscale 2013, 5, 5312.
NMC/Co@CNTs	500	79	Langmuir 2018, 34, 1992.
Ni-Co-O cages	380	50	Adv. Mater. 2016, 28, 4601.
CoP/rGO	340	66	Chem. Sci. 2016,7, 1690.
Co_9S_8(600)/N,S-GO	400	96	ACS Catal. 2015, 5, 3625.
Co_2P/CoFoil	319	79	J. Mater. Chem. A 2017, 5, 10561.

P-doped-Co@NC-3	340	85	*Adv. Funct. Mater.* 2019, 30, 1906081.

η = Overpotential; NA = not attained.

Table S3. The Comparison of HER performance of the Co-based material catalysts from the recent literature and this work (1 M KOH medium).

Catalysts	**η@10 mA/cm^2 (mV)**	**Tafel slop (mV/ dec)**	**Reference**
Co/N-CNTs-2	89	143	This work
Co/CoP–NC	260	104	Mater. Horiz., 2018, 5, 108
CoPx@CNS	91	129	Angew. Chem. Int. Ed. 2020, 59, 21360.
Co_2P/CoNPC	208	84	Adv. Mater. 2020, 2003649
Co-P film	94	42	Angew. Chem. Int. Ed. 2015, 54, 6251.
CoP/CC	209	129	J. Am. Chem. Soc. 2014, 136, 7587.
CoP-2ph-CMP-800	360	121	Chem. Commun., 2016, 52, 13483.
$Cu_{0.3}Co_{2.7}P$/NC	220	122	Adv. Energy Mater. 2017, 7, 1601555.
Co-NRCNTs	370	NA	Angew. Che., Int. Ed. 2014, 53, 4372.
Co-P-300	280	94	Chem. Commun. 2016, 52, 1633.
CoP NPs/CNSs	115	92	RSC Adv. 2019, 9, 39951.
CoP nanowire arrays	209	129	Nanoscale, 2014, 6, 13440.
CoOx/CN	232	NA	J. Am. Chem. Soc. 2015, 137, 2688.

Co-PCNFs	249	92	J. Mater. Chem. A 2016, 4, 12818.
Co/CNFs (1000)	190	66	Adv. Mater. 2019, 1808043
Co/CoP-3	320	95	Adv. Energy Mater. 2017, 7, 1602355.
Co@N-C	210	108	J. Mater. Chem. A 2014, 2, 20067.
Co@N-CNTs@rGO	108	55	Adv. Mater. **2018**, 30, 1802011.
CoP@BNC	215	52	Adv. Energy Mater. 2017, 7, 1601671.
Co_1/PCN	89	58	Nature Catalysis **2018**, 2, 134.
CoP nanowire array	209	129	J. Am. Chem. Soc. 2014, 136, 7587.
Co@NG	220	112	Adv. Funct. Mater. 2016, 26, 4397.

η = Overpotential; NA = not attained.